

Navigating the Red Planet: Comprehensive Analysis of the Martian Environment Through Innovative Drone Technology

Colby Davis
Department of Aerospace
Engineering
Embry-Riddle Aeronautical
University
Daytona Beach, United States
davic112@my.erau.edu

Renata Jancsik
Department of Aerospace
Engineering
Embry-Riddle Aeronautical
University
Daytona Beach, United States
jancsikr@my.erau.edu

David Scolare
Department of Aerospace
Engineering
Embry-Riddle Aeronautical
University
Daytona Beach, United States
scolared@my.erau.edu

Sarah Voss
Department of Aerospace
Engineering
Embry-Riddle Aeronautical
University
Daytona Beach, United States
vosss1@my.erau.edu

This process is intended to design a propeller-based drone that will analyze the surface of Mars and return information about the Martian environment. Following in the footsteps of the *Ingenuity* drone, this rotor-craft will carry equipment that can image the Martian Terrain and analyze the effects of Martian dust on its components. Many difficult aspects must be accounted for when designing such a craft, including the much lower density of air and wide variety of temperatures the craft must be able to endure. In this proposal, the preliminary aspects of design and control have been identified for further research and analysis, and a preliminary timeline for future work has been proposed.

I. Introduction

In April of 2021, the NASA Ingenuity helicopter performed the first controlled flight on the surface of another planet, flying for 39.1 seconds over the surface of Mars. This groundbreaking feat has opened the door to countless possibilities for future exploration of atmospheric planets.

Drones provide an entire new axis of freedom in regards to extraterrestrial exploration. Where rovers would typically get stuck because of terrain, a drone can simply fly over the top with ease. Building off Ingenuity's proof of concept, the goal is to now optimize the design and look to expand the scientific handiness of future Martian rotorcraft.

In light of this challenging problem, several critical research questions arise:

What is the optimal design for a rotor-based drone for the Martian atmosphere?

How can the components be designed to withstand the harsh environment?

What control mechanisms or algorithms are necessary to ensure a stable flight?

The proposed idea holds significant importance for the future of Martian exploration. By designing a propeller-base drone capable of high fidelity surface analysis, it can unlock new insights into geology, climate or habitability. Thus helping future manned missions to Mars, guiding the selection of landing sites.

II. Theoretical Development

The thin Martian atmosphere, approximately 1% of Earth's atmospheric density, pressure, gravity and temperature all pose an extreme challenge for flight and simulation. For this reason unique approaches are needed to test flight dynamics, such as dynamic scaling of the model or gravity off-loading [2].

Using the equations below, the required force needed to lift off on Mars using a single propeller was determined. Subsequently, the theoretical lift of the initial design drone was found to ensure mission feasibility.

$$T = C_T \rho A \Omega^2 \quad (1)$$

$$T = ma \quad (2)$$

Table 1: Lift on Mars vs Earth

Lift	Mars	Earth
Required	5.57 N	14.7 N
Theoretical	2.23×10^3 N	1.44×10^5 N

The numbers in Table 1 were found using the initial design choices of a mass of 1.5 kg and 4500 RPM for the propellers. Meaning that the drone needs to create at least 1.44×10^5 N on Earth to take off on Mars.

Another problem is poor aerodynamic damping due to the thin atmosphere causing flapping of the wings, however, due to mathematical analysis most research is done using rigid blade analysis. The derivation for rigid body flapping is too long to be explained in this report but it is determined by balancing the moments of aerodynamic and inertial forces around a hinge which can be seen in Fig. 1.

Counter-Clockwise:

$$k_\beta(\beta - \beta_P) = \int_0^R r dF_\beta - \int_0^R (mr\ddot{\beta} dr) r - \int_0^R (m\Omega^2 r dr) r \beta - \int_0^R m\ddot{\alpha}_x r^2 \sin \psi dr \\ + \int_0^R m\ddot{\alpha}_y r^2 \cos \psi dr - \int_0^R 2(mr^2 dr) \dot{\alpha}_x \Omega \cos \psi \\ - \int_0^R 2(mr^2 dr) \dot{\alpha}_y \Omega \sin \psi - \int_0^R m\ddot{z}_h r dr \quad (2.2)$$

Clockwise:

$$k_\beta(\beta - \beta_P) = \int_0^R r dF_\beta - \int_0^R (mr\ddot{\beta} dr) r - \int_0^R (m\Omega^2 r dr) r \beta + \int_0^R m\ddot{\alpha}_x r^2 \sin \psi dr \\ + \int_0^R m\ddot{\alpha}_y r^2 \cos \psi dr + \int_0^R 2(mr^2 dr) \dot{\alpha}_x \Omega \cos \psi \\ - \int_0^R 2(mr^2 dr) \dot{\alpha}_y \Omega \sin \psi - \int_0^R m\ddot{z}_h r dr \quad (2.3)$$

Fig. 1. Equation of Motion for Rigid Blade Flapping Model [1].

Using equations of motion for three translational equations and three rotation equations, the state space model can be derived which can be seen in Fig. 2.

$$X = m(\dot{u} + qw - rv) + mg \sin \theta$$

$$Y = m(\dot{v} + ru - pw) - mg \cos \theta \sin \phi$$

$$Z = m(\dot{w} + pv - qu) - mg \cos \theta \cos \phi$$

$$L = I_{xx}\dot{p} - I_{xz}(\dot{r} + pq) - (I_{yy} - I_{zz})qr$$

$$M = I_{yy}\dot{q} - I_{xz}(r^2 - p^2) - (I_{zz} - I_{xx})pr$$

$$N = I_{zz}\dot{r} - I_{xz}(\dot{p} - qr) - (I_{xx} - I_{yy})pq$$

Fig. 2. State State Equations for Translational and Rotational Movement [1].

For a drone moving in a 3D space, there needs to be more information to allow for control which is made up by a set of kinematic angle relations shown in Fig. 3.

$$\dot{\phi} = p + q \frac{\sin \theta \sin \phi}{\cos \theta} + \frac{r}{\sin \theta \cos \phi} \cos \theta$$

$$\dot{\theta} = q \cos \phi - r \sin \phi$$

$$\dot{\psi} = q \frac{\sin \phi}{\cos \theta} + r \frac{\cos \phi}{\cos \theta}$$

Fig. 3. State State Equations for Translational and Rotational Movement [1].

Finally, all these parts must be organized into the standard state space form with A and B matrices shown in Fig. 4. The primary objective of this project is to hover, which will be done by satisfying the states of the system the with condition $\phi_0 = \theta_0 = \psi_0 = 0$, which will need to be done using the fastest yet effective response from a controller. Ultimately, the selection of an optimal controller will need to be done through testing and tuning. The most promising controllers that will be tested are PID(Proportional-Integral-Derivative), MPC (Model Predictive Control), and state-space feedback.

$$\begin{aligned}
\begin{bmatrix} \Delta \dot{u} \\ \Delta \dot{v} \\ \Delta \dot{w} \\ \Delta \dot{p} \\ \Delta \dot{q} \\ \Delta \dot{r} \\ \Delta \dot{\phi} \\ \Delta \dot{\theta} \\ \Delta \dot{\psi} \end{bmatrix} &= \begin{bmatrix} X_u & X_v & X_w & X_p & X_q & X_r & 0 & -g \cos \theta_0 & 0 \\ Y_u & Y_v & Y_w & Y_p & Y_q & Y_r & g \cos \theta_0 \cos \phi_0 & -g \sin \theta_0 \sin \phi_0 & 0 \\ Z_u & Z_v & Z_w & Z_p & Z_q & Z_r & -g \cos \theta_0 \sin \phi_0 & -g \sin \theta_0 \cos \phi_0 & 0 \\ L_u & L_v & L_w & L_p & L_q & L_r & 0 & 0 & 0 \\ M_u & M_v & M_w & M_p & M_q & M_r & 0 & 0 & 0 \\ N_u & N_v & N_w & N_p & N_q & N_r & 0 & 0 & 0 \\ 0 & 0 & 0 & 1 & \frac{\sin \theta_0 \sin \phi_0}{\cos \theta_0} & \frac{\sin \theta_0 \cos \phi_0}{\cos \theta_0} & 0 & 0 & 0 \\ 0 & 0 & 0 & 0 & \cos \phi_0 & -\sin \phi_0 & 0 & 0 & 0 \\ 0 & 0 & 0 & 0 & \frac{\sin \phi_0}{\cos \theta_0} & \frac{\cos \phi_0}{\cos \theta_0} & 0 & 0 & 0 \end{bmatrix} \begin{bmatrix} \Delta u \\ \Delta v \\ \Delta w \\ \Delta p \\ \Delta q \\ \Delta r \\ \Delta \phi \\ \Delta \theta \\ \Delta \psi \end{bmatrix} \\
&+ \begin{bmatrix} X_{u0} & X_{uc} & X_{us} & X_{l0} & X_{lc} & X_{ls} \\ Y_{u0} & Y_{uc} & Y_{us} & Y_{l0} & Y_{lc} & Y_{ls} \\ Z_{u0} & Z_{uc} & Z_{us} & Z_{l0} & Z_{lc} & Z_{ls} \\ L_{u0} & L_{uc} & L_{us} & L_{l0} & L_{lc} & L_{ls} \\ M_{u0} & M_{uc} & M_{us} & M_{l0} & M_{lc} & M_{ls} \\ N_{u0} & N_{uc} & N_{us} & N_{l0} & N_{lc} & N_{ls} \\ 0 & 0 & 0 & 0 & 0 & 0 \\ 0 & 0 & 0 & 0 & 0 & 0 \\ 0 & 0 & 0 & 0 & 0 & 0 \end{bmatrix} \begin{bmatrix} \Delta \theta_{u0} \\ \Delta \theta_{uc} \\ \Delta \theta_{us} \\ \Delta \theta_{l0} \\ \Delta \theta_{lc} \\ \Delta \theta_{ls} \end{bmatrix} \quad (2.44)
\end{aligned}$$

Fig. 4. State Space Matrices for Coaxial Drone [1].

III. Preliminary Simulation and Control

For the purposes of this simplified design, the complexities of the system were significantly reduced to begin modeling and simulation. The ultimate goal of starting with an extremely simplified model in the beginning of the simulation process would be to gradually build up the complexity of the model until a reasonably accurate representation of system dynamics is achieved.

In order to assess the preliminary accuracy of the simulation, the thrust was modeled using Equations 3 and 4, where S is the circular area swept by the propeller in m^2 and Ω is the rotational speed of the propeller in RPM [10].

$$T = \frac{1}{2} \rho S [V_1^2 - V_0^2] \quad (3)$$

$$V_1 = 2\pi * r * \Omega * \tan \alpha \quad (4)$$

These equations were modeled in Simulink to generate simulated thrust curves to compare with experimental data from Earth and assess the accuracy of this model. In this case, the area swept by the propeller and the radius were affected by the large variable pitch mechanism (whose design is specified in Section IV), which most likely contributed to the generation of higher ideal thrust than expected. The shape of the airfoil on the propeller, the mass

of the potential rotorcraft, and gravity are also unaccounted for in this model. The inclusion of these specificities, most specifically using an elemental analysis of airfoil shape [14], would improve the accuracy of this model greatly.

This model also includes preliminary calculations of motor torque, which must be counteracted in order to maintain system stability. Torque was calculated using Equation 5 [], which is a simplified torque calculation that again does not account for the shape of the airfoil or the pitch of the propeller.

$$\tau = 5252 * \frac{HP}{\Omega} \quad (5)$$

The preliminary Simulink model is shown in Figures 5 and 6, and a more complex Simulink model of a variable pitch propeller system is shown in Figure 7.

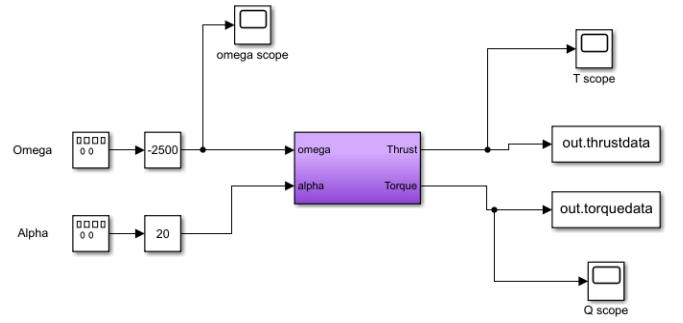


Fig. 5. Simulink model of preliminary thrust and torque.

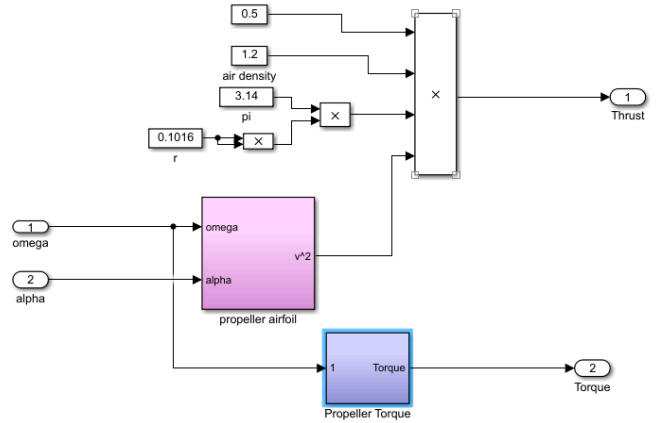


Fig. 6. Modeling of equations in the subsystem block shown in Figure 5.

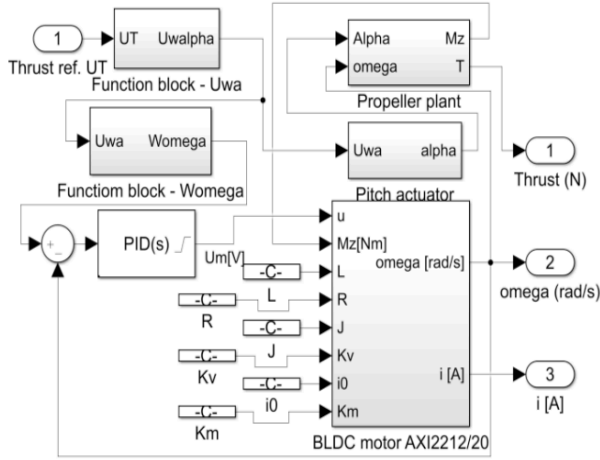


Fig. 7. Example of a more complex model of variable pitch control in Simulink [9].

Using the Simulink model shown in Figures 5 and 6, several simulations were run at varying pitch angles and motor rotational speeds to collect preliminary data for comparison to experimental data and determine model accuracy. Pitch angles were varied between 3° and 20° , where diminishing returns were expected after 15° [3]. Motor speeds were varied between 2500 RPM and 5000 RPM. Thrust curves were generated using both the density of air at MSL on Earth (1.2 kg/m^3) and an average air density on Mars (0.02 kg/m^3) [8]. This data is summarized in Figures 8 - 12, and experimental thrust data for a miniaturized variable pitch propeller on Earth is shown in Figure 13.

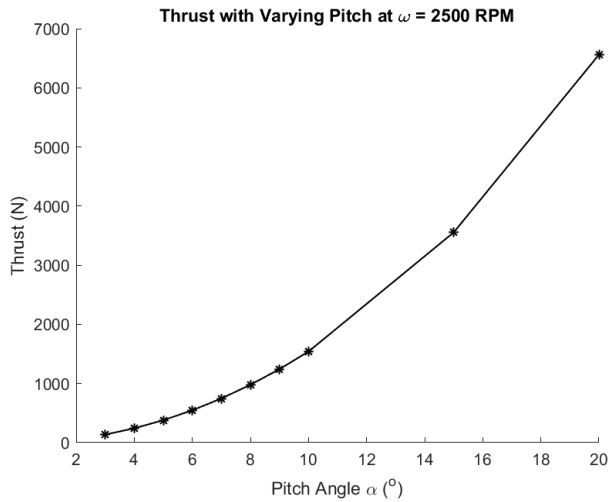


Fig. 8. Simulation data for varying pitch of the modeled system at 2500 RPM on Earth.

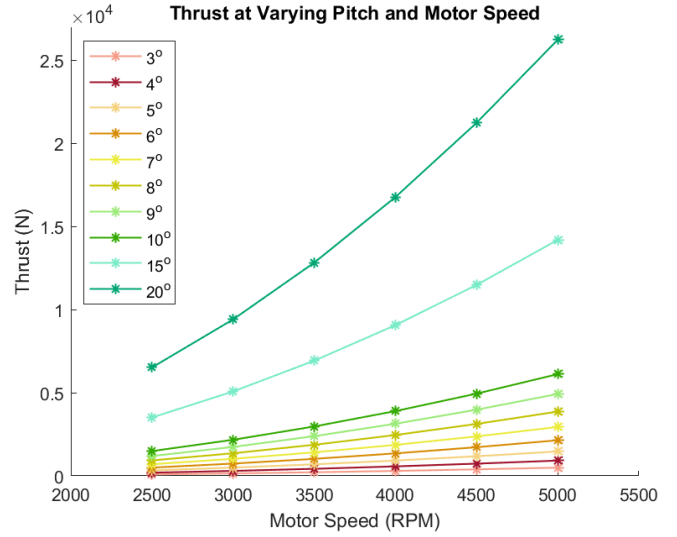


Fig. 9. Simulation data for varying pitch and varying motor rotational speeds on Earth.

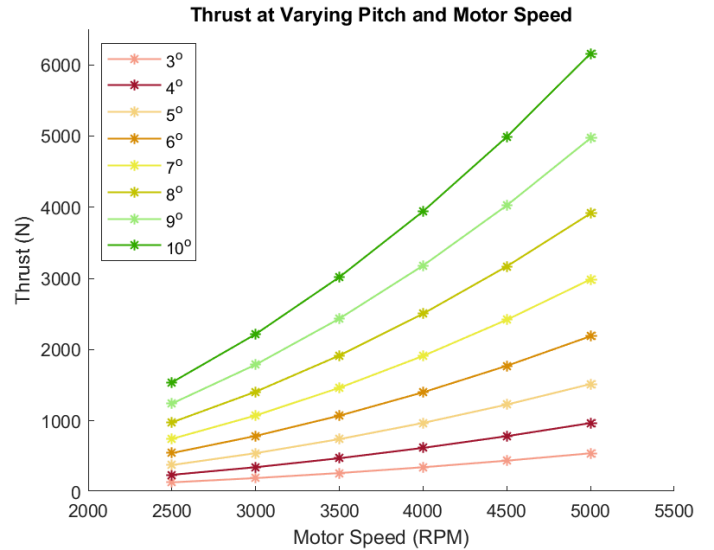


Fig. 10. Simulation data for varying pitch and varying motor rotational speeds on Earth where pitch angles of 15° and 20° have been removed to analyze data more precisely.

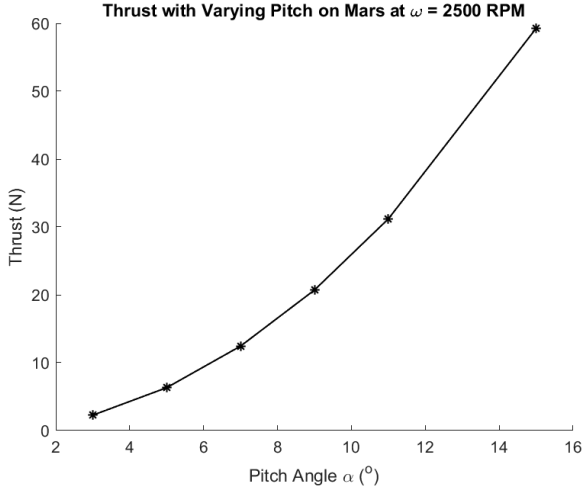


Fig. 11. Simulation data for varying pitch of the modeled system at 2500 RPM on Mars, where fewer pitch angles were analyzed for simplicity.

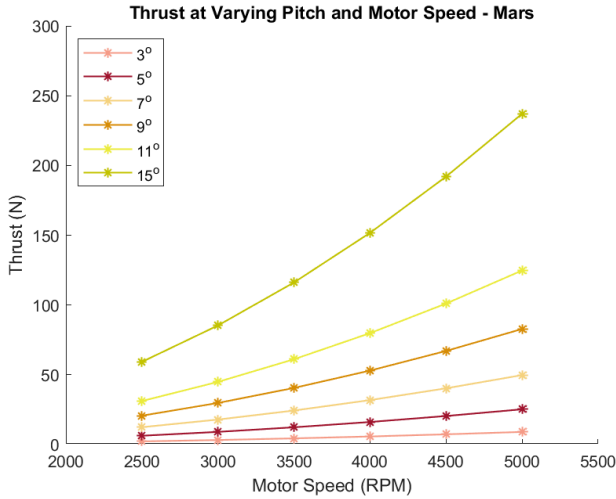


Fig. 12. Simulation data for varying pitch and varying motor rotational speeds on Mars.

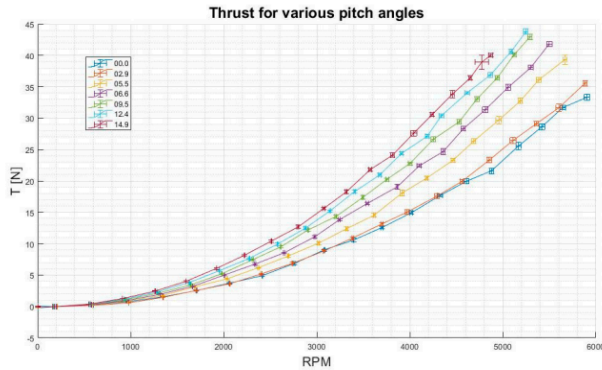


Figure 5. Thrust for various pitch angles.

Fig. 13. Experimental thrust data for a variable pitch propeller at varying rotational speeds [3].

As seen in Figures 5 and 7, the Simulink model created has not yet modeled the motor dynamics, which would be the next step in the development of this model. The motor dynamics, specifically the voltage, would be used in the preliminary control of this system's rotational speed and pitch angle. Once the motor dynamics have been modeled, a preliminary controller would be implemented to begin testing the system, in this case a PID controller. As stated previously, the true system dynamics are quite complex, and for a small-scale rotorcraft to be controlled and tested a state-space based control algorithm would need to be used to capture system complexities as accurately as possible. Figure 14 shows a block diagram of the ideal simplified system controller after motor dynamics are determined and modeled.

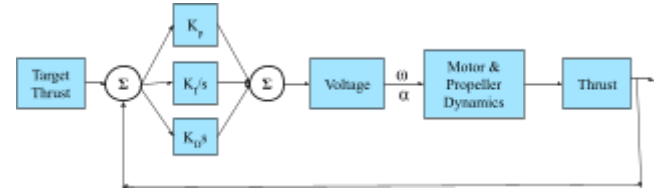


Fig. 14. Early block diagram of a PID controller for the system.

IV. Design and Modeling

The ideal design for this system would be a coaxial drone, where each rotor has a variable pitch mechanism. For the purposes of this assignment, a single variable rotor was used, leaving the design and control of a coaxial system as a long-term goal. Variable pitch rotors have been shown [3] to increase the amount of thrust produced by a given rotor and were used in the design of the *Ingenuity* drone [1]. In order to appropriately test the proposed design, the design must be small enough to reasonably 3D print, and be designed so that enough thrust is produced to theoretically hover the motor, rotor, and controller system.

IV.1 Rotor System

For the purposes of this design, the propeller blades shall be 3D printed and must be scaled down to fit in a standard sized printer bed [6]. The propeller blades will be modeled after the Fluxer VTOL 16.1”*6.4” blades [7], which have been used for similar experiments before [3] and are small enough to fit within the limitations of a 3D printer bed with some slight adjustments.

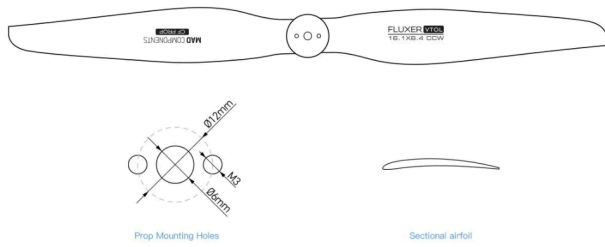


Fig. 15. Cross-sectional shape and other dimensions of Fluxer VTOL Propeller blade [7].

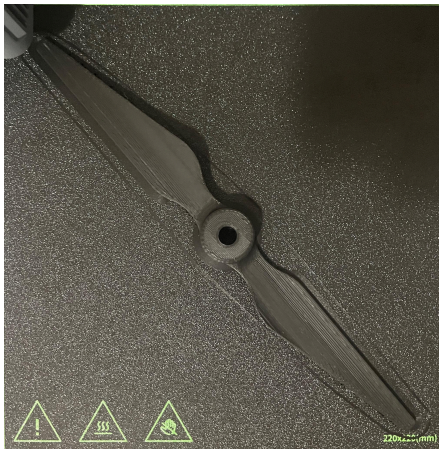


Fig. 16. Test Print of initial Propeller Design using PLA+

IV.2 Motor System

A small VTOL motor will be used to power the blades, along with a 3D printed gear subassembly to control the coaxial spin of both of the rotors. Trade studies will be conducted to determine a motor of appropriate size and capabilities for use in this project.

IV.4 Raspberry Pi

Using a Raspberry Pi enables the management of both the motors and flight controllers. This is achieved by writing the control algorithm to the Pi, establishing a connection between the motors and the Pi, and subsequently linking the control algorithm to the motor. Finally, a receiver will be integrated to enhance communication with the drone.

V. Testing Variable Pitch

V.1 Subassembly Body

To keep the test lightweight and inexpensive there were several 3D printed parts. The propellers along with the body and motor connection were made from PLA+.

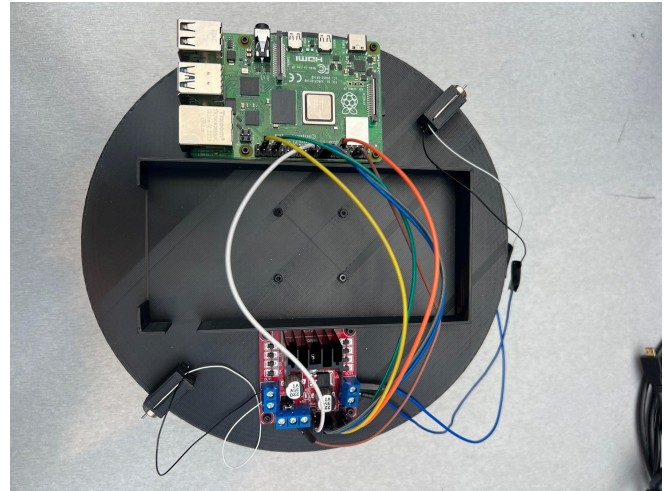


Fig. 17. Disc Subassembly

V.2 Electrical System

Using an onboard 15000 mAh portable battery both the L298N and Raspberry Pi 4 were powered using USB cables.

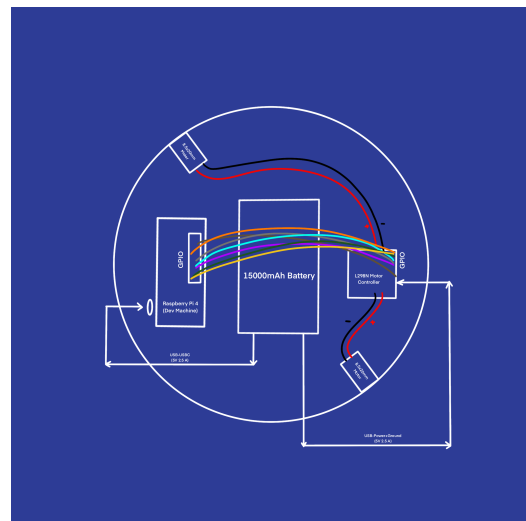


Fig. 18. Variable Pitch Electrical Schematic

As it can be seen above the L298N motor was connected to the Raspberry Pi and the pitch motors. The Raspberry Pi

connects with GPIO cables which are used to control the speed and direction of the motors. The technique used is called Pulse Width Modulation (PWM) which by varying the cycle sent to the motors the speed can be controlled.

V.3 Variable Pitch Mechanism

For a full size drone typical variable pitch mechanisms consist of actuators, gears, brushings and many more moving parts. This increased complexity comes with a decrease in volume but an increase in cost. For this reason initial testing of pitch angle was controlled using two small motors.

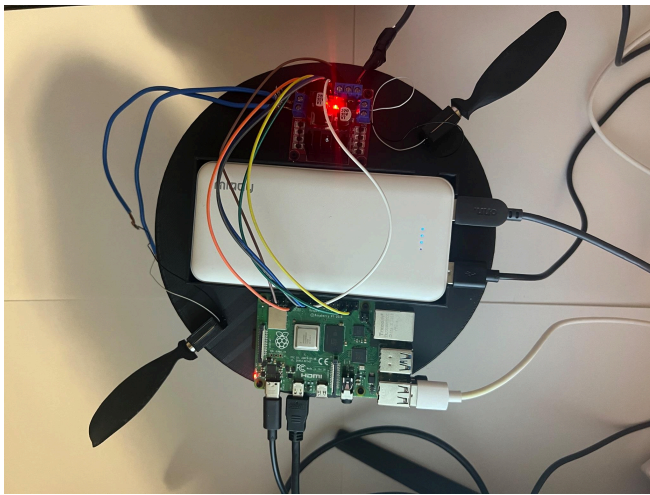


Fig. 19. Propeller Blades Attached to 8.5x20mm Motors

VI. Future Improvements

To start, the Raspberry Pi will be connected to a Dev Machine through wifi, allowing for commands to be sent remotely to the system instead of being accessed through the onboard computer (OBC). Through this wireless connection an inertial measurement unit (IMU) can be connected to the Raspberry Pi and information can be sent to the Dev Machine allowing for feedback control. Ideally using machine learning a state space model will be established to perform flight dynamics from this information.

Lastly, the main motor and variable pitch mechanism will be integrated together allowing for the full size propellers. This is a more complex step but will greatly decrease the volume of the overall build as seen in Fig. 20.

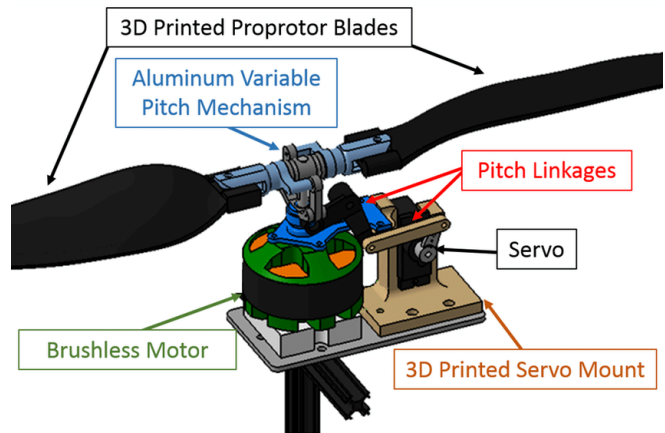


Fig. 20. Integrated Variable Pitch and Motor [13]

VII. Project Schedule

Once understanding the key assumptions for this project including the Martian environment, the first step of this process is to design and 3D print an optimal propeller. The initial testing of a variable pitch propeller proved successful, leading us to build a more complex design in the future. Upon completion, there should be a general idea of how to move forward regarding the motor of the system as well as other components like the landing gears. Having found the new hardware components, it should be plausible to have a fully completed CAD modeled by August 2024.

Once the physical system is complete, the group work deviates into two parts; working on connecting the physical system to the Arduino to ensure optimal control performances, and performing tests in ANSYS to ensure a successful mission for the drone.

The preliminary simulation and control proved successful, exceeding the needed thrust to take off on mars. All that remains is to create a control algorithm allowing the propeller/motor system to hover, which is planned to be completed by September 2024.

VIII. Acknowledgment

The authors of this report acknowledge the valuable input and expertise shared by our instructor Dr. Sergey Drakunov, as well as the gracious assistance from his lab in acquiring necessary hardware in the building of our physical model.

IX. References

- [1] E. Greenbaum, "Flight Dynamics of a Coaxial Helicopter Hovering on Mars." Order No. 30491648, University of Maryland, College Park, United States -- Maryland, 2023.
- [2] M. Veismann, C. Dougherty, J. Rabinovitch, A. Quab, M. Gharib. 2021. "Low-density multi-fan wind tunnel design and testing for the Ingenuity Mars Helicopter." *Experiments in Fluids*, 62(193) <https://doi.org/10.1007/s00348-021-03278-5>
- [3] M. Podsekowski, R. Konopinski., D. Obidowski, and K. Koter. 2020. "Variable pitch propeller for UAV - Experimental tests." *Energies*, 13(20). <https://www.mdpi.com/1996-1073/13/20/5264>
- [4] Propelleradmin. 2023. "Drone surveying: Why it's important and how it works." *Propeller*. <https://www.propelleraero.com/blog/drone-surveying-why-its-important-and-how-it-works/#:~:text=Because%20drones%20can%20fly%20at,than%20a%20base%20and%20rover.>
- [5] R. D. Lorenz. 2022. "Planetary Exploration with Ingenuity and Dragonfly." *American Institute of Aeronautics and Astronautics*. <https://arc.aiaa.org/doi/epub/10.2514/4.106378>
- [6] TH3D Studio. "Printer Bed Sizing chart." <https://support.th3dstudio.com/helpcenter/printer-bed-sizing-chart/>
- [7] UnmannedRC. "Fluxer VTOL Prop 16.1"*6.4". " <https://unmannedrc.com/products/fluxer-vtol-prop-16-1x6-4-inch>
- [8] Grip, H.F., Johnson, W., Malpica, M. et al. (2020). "Modeling and identification of hover flight dynamics for NASA's Mars helicopter." *Journal of Guidance, Control, and Dynamics*. 43(2). <https://doi.org/10.2514/1.G004228>
- [9] Gebauer, J., Wagnerova, R., Smutny, P., and Podesva, P. (2019). "Controller design for variable pitch propeller propulsion drive." *International Federation of Automatic Control*, 52(27). <https://doi.org/10.1016/j.ifacol.2019.12.754>
- [10] Gebauer, J., and Koci, . (2013). "The electronic variable pitch drive." *Instruments and Control Seminar VSB-TUO*.
- [11] Imamura, A., Masafumi, M., and Hino, J. (2016). "Flight characteristics of quad rotor helicopter with thrust vectoring equipment." *Journal of Robotics and Mechatronics*, 28(3). <https://doi.org/10.20965/jrm.2016.p0334>
- [12] Calculator Academy. (2023). "Propeller Torque Calculator." <https://calculator.academy/propeller-torque-calculator/>
- [13] Phillips, B., Hrishikeshavan, V., & Chopra, I. (2018). Enhancing the Performance of a Quadrotor Biplane Tail-sitter (QBiT).
- [14] MIT. () "Performance of propellers." <https://web.mit.edu/16.unified/www/FALL/thermodynamics/notes/node86.html>